

**Fabrication of necklace-like fibers separator by electrospinning technique for
high electrochemical performance and safe lithium metal batteries**

Can Liao, Longfei Han, Na Wu, Xiaowei Mu, Yuan Hu ,Yongchun Kan*, Lei Song *

State Key Laboratory of Fire Science, University of Science and Technology of

China, Hefei, Anhui 230026, PR China

*Corresponding author.

E-mail address: yckan@ustc.edu.cn (Y. Kan); leisong@ustc.edu.cn (L. Song).

1. Experiment section

1.1 Raw materials

Tetraethyl orthosilicate (TEOS, >99 %, AR), absolute ethanol (>99 %, AR) and ammonia solution ($\text{NH}_3 \cdot \text{H}_2\text{O}$, >99 %, AR) were purchased from Sinopharm Chemical Reagent Co., Ltd. Polyvinyl alcohol (PVA-1799) and 1-Methyl-2-pyrrolidinone (NMP, >99.5 %, AR) were provided by Aladdin Biochemical Technology Co., Ltd. The separator of Celgard 2325, as one of the most common commercialization separator, was supplied by the Celgard company of America. The cathode active material of LiFePO_4 powder was purchased from BTR New Energy Material Ltd, and the anode of lithium metal foil with the thickness of 0.5 mm (>99.5 %, purity) was offered by China Energy Lithium Co., Ltd. The conductivity agent of acetylene black and the binder of PVDF powder (battery level) were provided by Saibo Agents Co. Ltd. The liquid electrolyte of 1.0 M LiPF_6 in ethylene carbonate (EC)/dimethyl carbonate (DMC) (1:1, v/v) was purchased from Dongguan Shanshan Battery Materials Co., Ltd.

1.2 The preparation of PVA@ SiO_2 spindle-knots structure separator

Firstly, we synthesize SiO_2 microspheres through the classic stober method. Pour 300 ml of absolute ethanol, 20 ml of $\text{NH}_3 \cdot \text{H}_2\text{O}$ and 20 ml of deionized water into the three-necked flask in turn, and stir for 1 h to acquire the mixed solution. Then slowly add 60 ml of TEOS to the three-necked flask containing the mixed solution and stirred at room temperature for 12 h to obtain a milky white suspension. The suspension was then centrifuged at high speed and washed repeatedly with ethanol until neutral. Finally, it is dried in 100 °C oven to obtain white powder of SiO_2 microspheres.

We used deionized water as the solvent and slowly stirred in a 90 °C water bath for 8 h to prepare a PVA solution with a mass fraction of 10 %. Then slowly add different masses of SiO₂ to obtain PVA-SiO₂ mixed solutions. Next, the solution is transformed into fiber separators by electrospinning under the condition of a voltage of 18 kV and a constant feed speed of 0.1 mm min⁻¹. Finally, the fiber separators were placed in an oven and heat treated under a certain pressure for 30 min to increase the strength. The separators prepared from solutions with PVA and SiO₂ mass ratios of 100:0, 90:10, 75:25 and 50:50 were named PVA, P@S-10, P@S-25 and P@S-50, respectively.

1.3 Separator characterization

Scanning electron microscope (SEM) was adopted to observe the microstructure morphology of SiO₂ particles, PVA fiber and lithium dendrites after Li dripping/stripping cycles. Thermal stability of separator was recorded by differential scanning calorimetry (DSC) thermograms under an atmosphere of nitrogen with a heating rate of 10 °C min⁻¹. The surface Young-modulus of separator was tested by atomic force microscope (AFM) by using the silicon probe of RTESP-525. The contact angle was measured by a SL200B contact angle system. Each sample was tested five times and then averaged.

The porosity is one of the most critical parameter of separator and is calculated by immersing the separator in n-butanol for half an hour, and then calculated by the following formula:

$$P(\%) = \frac{W_a - W_b}{\rho_b \times V_s}$$

where W_a and W_b express the weight of separator after and before immersing in n-butanol, respectively. ρ_b represent the density of n-butanol, and V_s is the volume of dry separator. The uptake of separator shows the capability of electrolyte retention, and it can be acquired by the follow equation:

$$T(\%) = \frac{W_w - W_d}{W_d}$$

where W_d represents the weight of dry separator. The W_w is the weight of wet separator after immersing liquid electrolyte for 30 min and then wiping off excess electrolyte with tissue. The ionic conductivity (σ) of separator was calculated by the follow equation:

$$\sigma = \frac{l}{R_b \times S}$$

where l and S represent the thickness and the effective area of dry separator, respectively. R_b is the bulk resistance of separator, which was measured by utilizing electrochemical impedance spectroscopy (EIS) at room temperature.

For measurements of electrochemical performance, the CR2032 coin cells were assembled in glove box ($O_2 < 0.1$ ppm, $H_2O < 0.1$ ppm). The cathode was composed of $LiFePO_4$, acetylene black and PVDF by the weight ratio of 8:1:1. For the comparison, the commercial separator of Celgard 2325 was also assembled and tested under the same conditions. The charge-discharge cycle was performed at the current density of 0.2C under the voltage range from 2.8 V to 4.2 V and the rate capability test was measured from 0.1C to 16C.

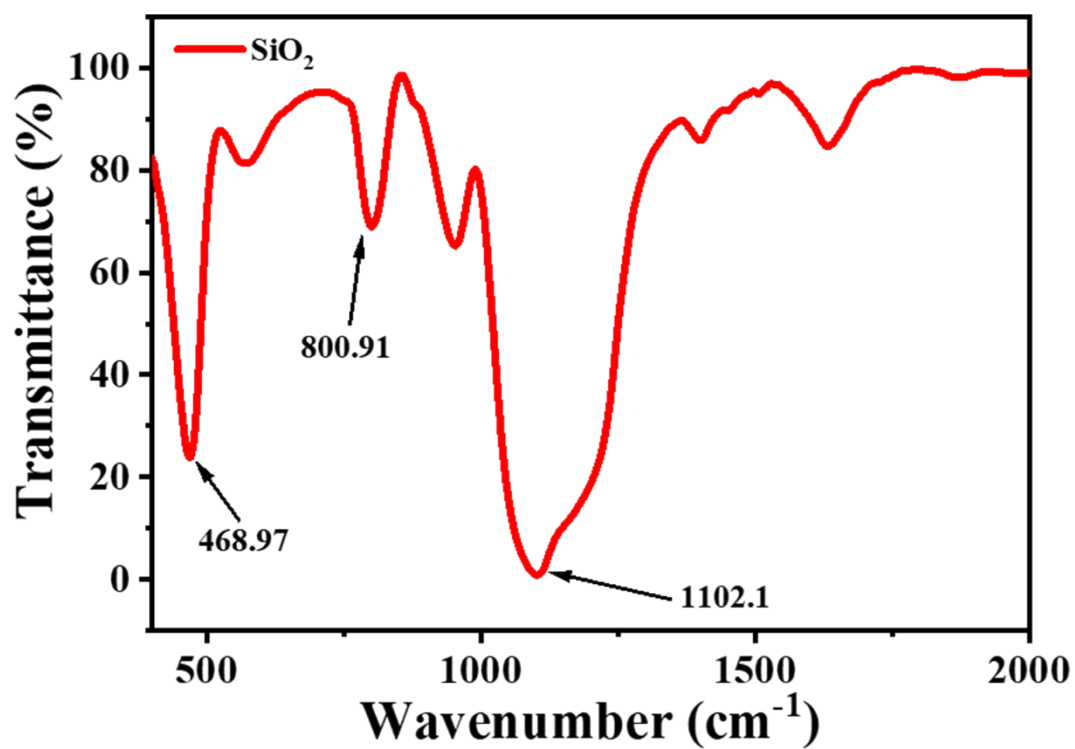
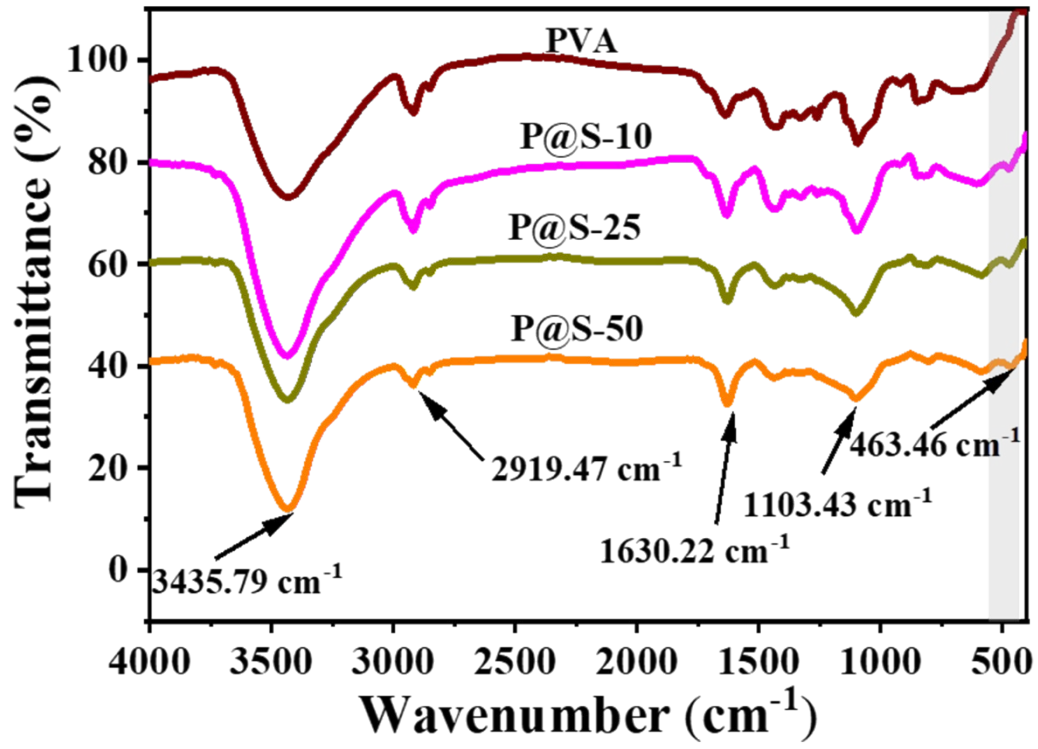


Figure S1. FT-IR curve of SiO₂ nanoparticles



Figure

re S2. FT-IR curve of PVA and P@S composite fibers.

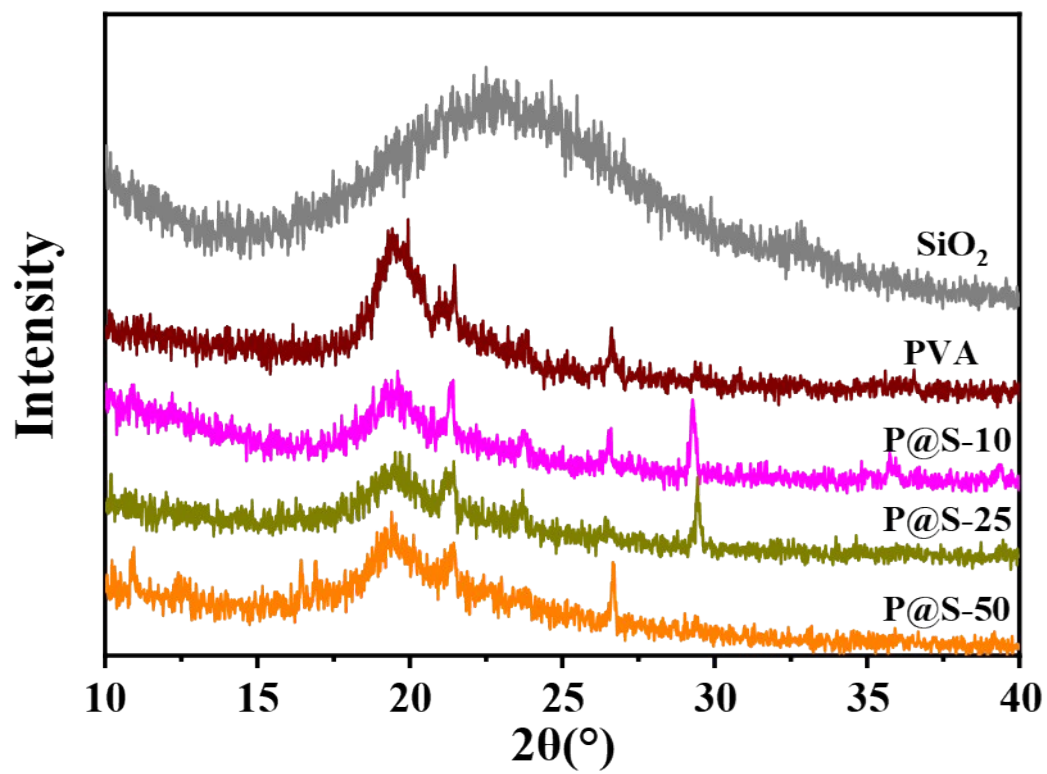


Figure. S3. XRD patterns of PVA and P@S composite fibers.

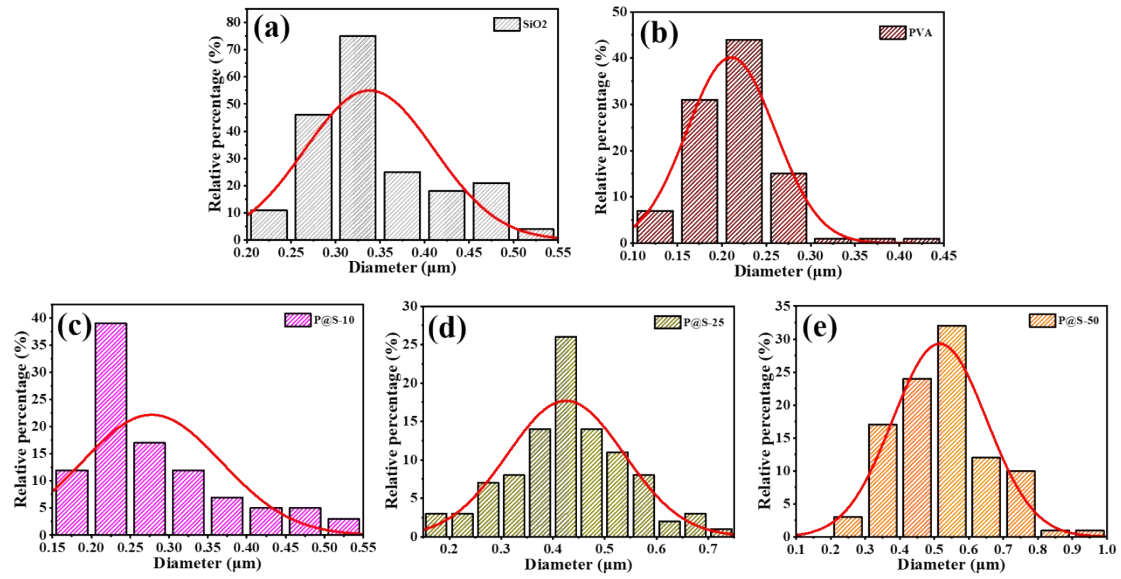


Figure. S4. The size distribution of SiO₂ particles and PVA@SiO₂ composite fibers. (a) SiO₂ particles; (b) PVA fibers; (c) P@S-10 fibers; (d) P@S-25 fibers; (e) P@S-50 fibers.

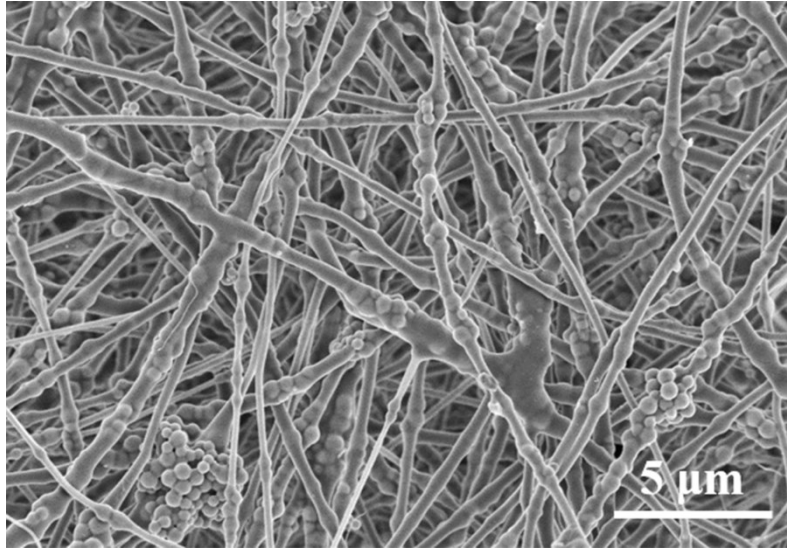


Figure S5. SEM images of P@S-50 separator with SiO₂ gathering.

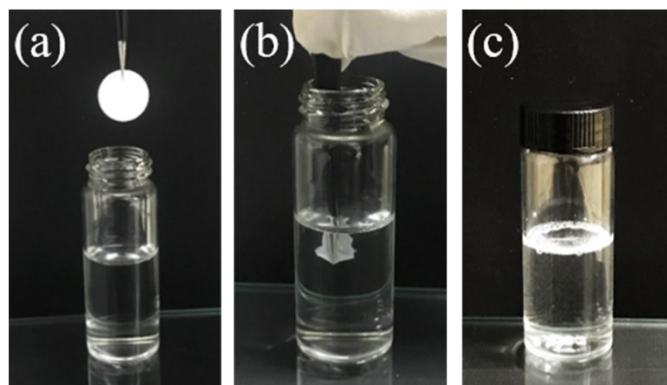


Figure S6. The P@S-50 separator environmental degradability test. (a) Before and (b) after immersing into tap water, and (c) after 30 min shaking.

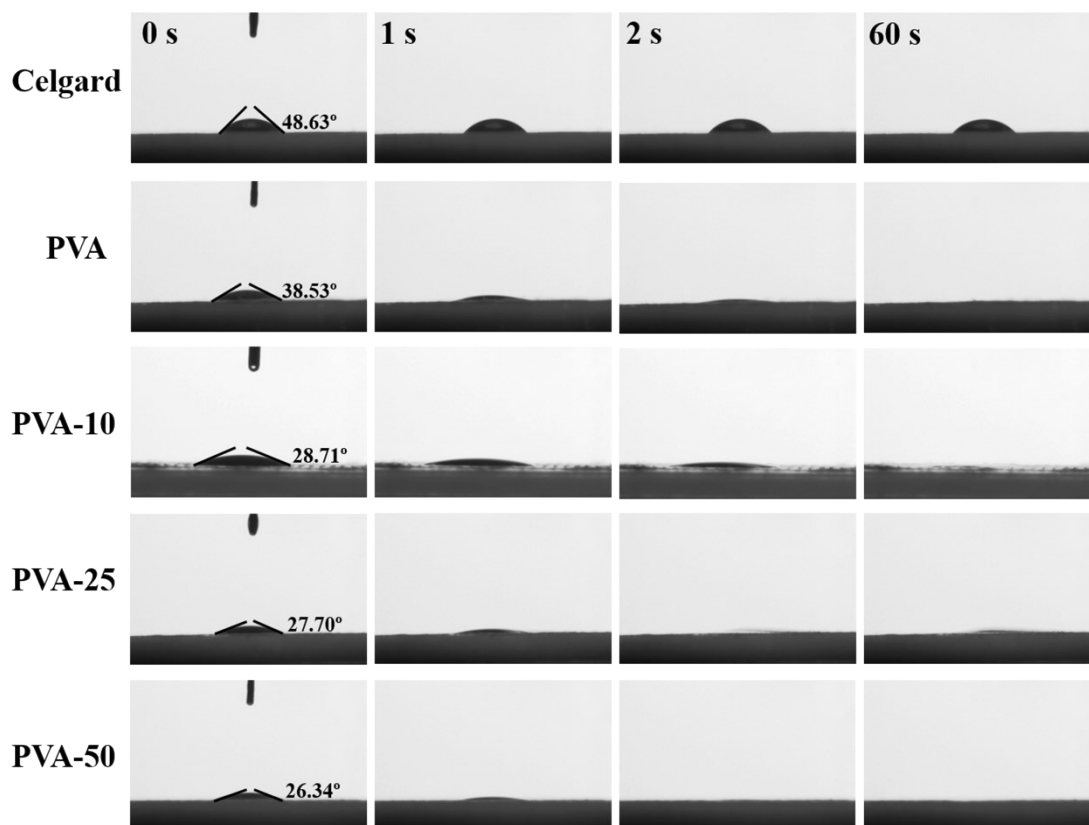


Figure S7. The contact angle test between various separator and electrolyte at which the droplet drops down for 0s, 1 s, 2 s, and 60 s. The liquid electrolyte of 1 M LiPF₆ in EC/DMC (v:v=1:1) was utilized.

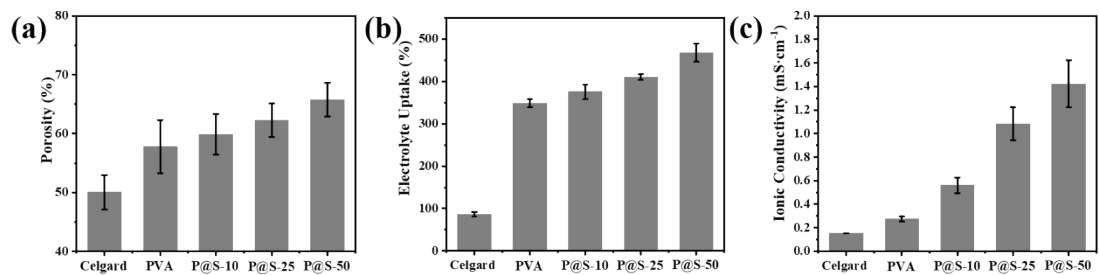


Figure S8. (a) The porosity, (b) the electrolyte uptake and (c) the ionic conductivity consequences of different separator. Each result was measured at least five times and then averaged.

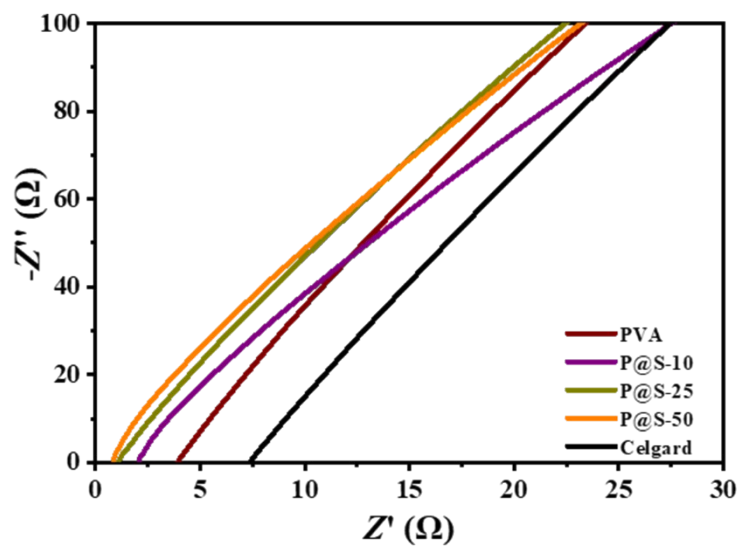


Figure S9. Nyquist impedance plot of various separator with the cell assembling with stainless steel//separator// stainless steel. The spectra were recorded over a frequency range from 0.01 to 10^6 Hz.

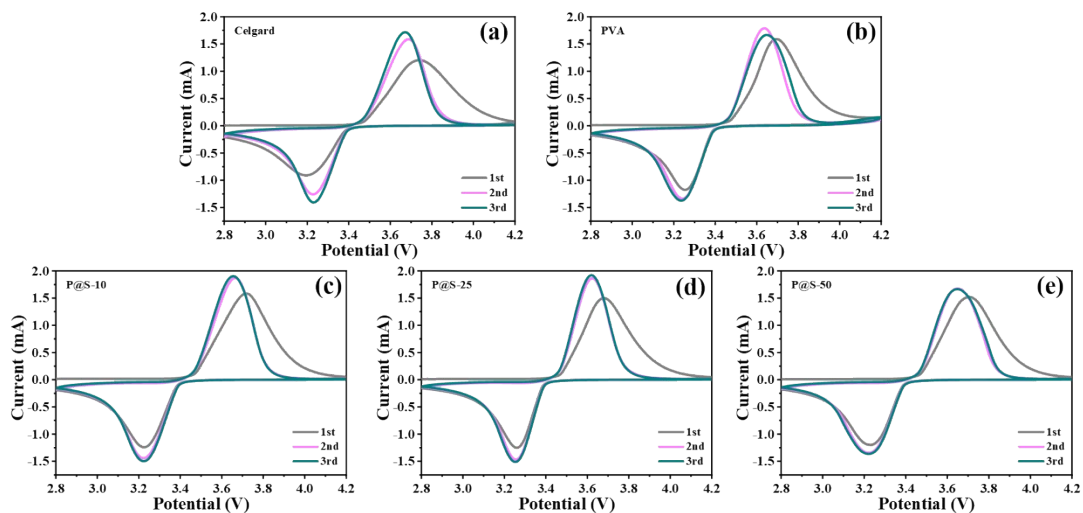


Figure S10. CV curves of cell by using various separator at the scan rate of 0.5 mV/s. (a) Celgard; (b) PVA; (c) P@S-10; (d) P@S-25; (e) P@S-50.

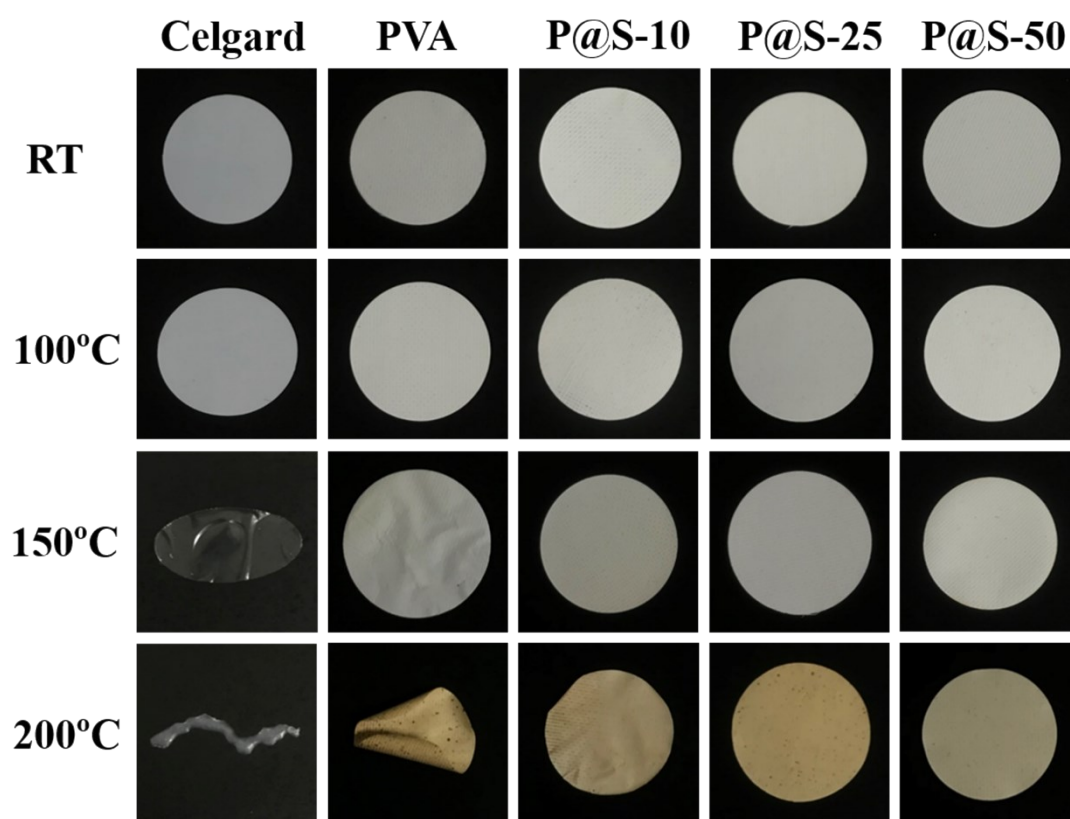


Figure S11. Thermal shrinkage test of separator at each temperature for 30 min.

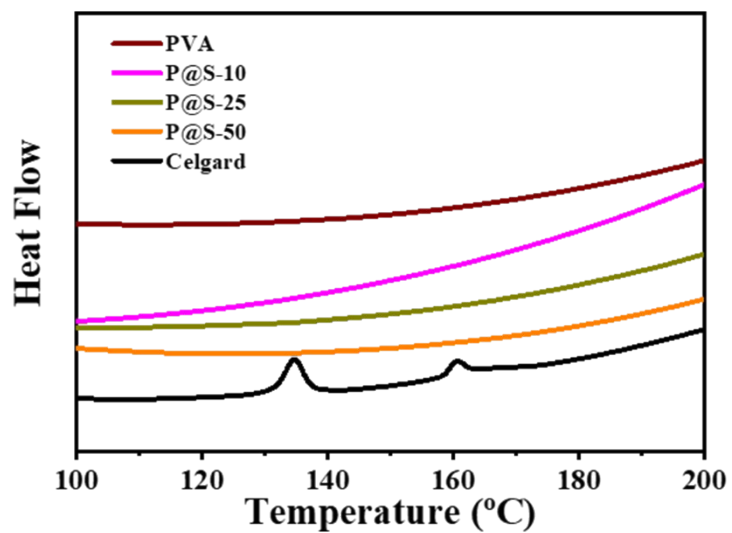


Figure S12. The DSC results of various separator at the heating rate of 10 min/°C.

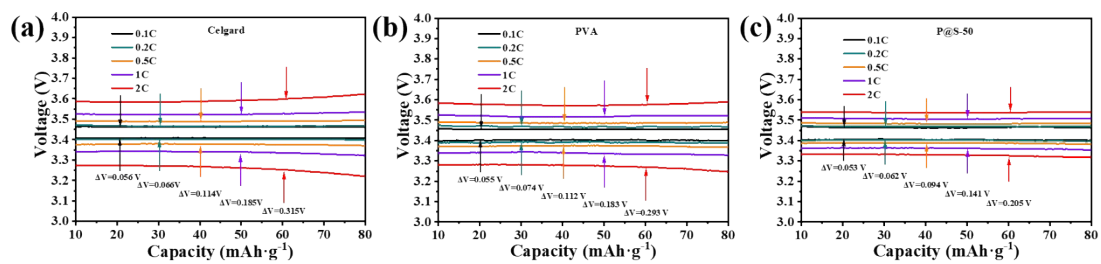


Figure S13. The magnification of voltage –capacity curve with current density from 0.1C to 2C. (a) Celgard separator, (b) PVA separator and (c) P@S-50 separator.

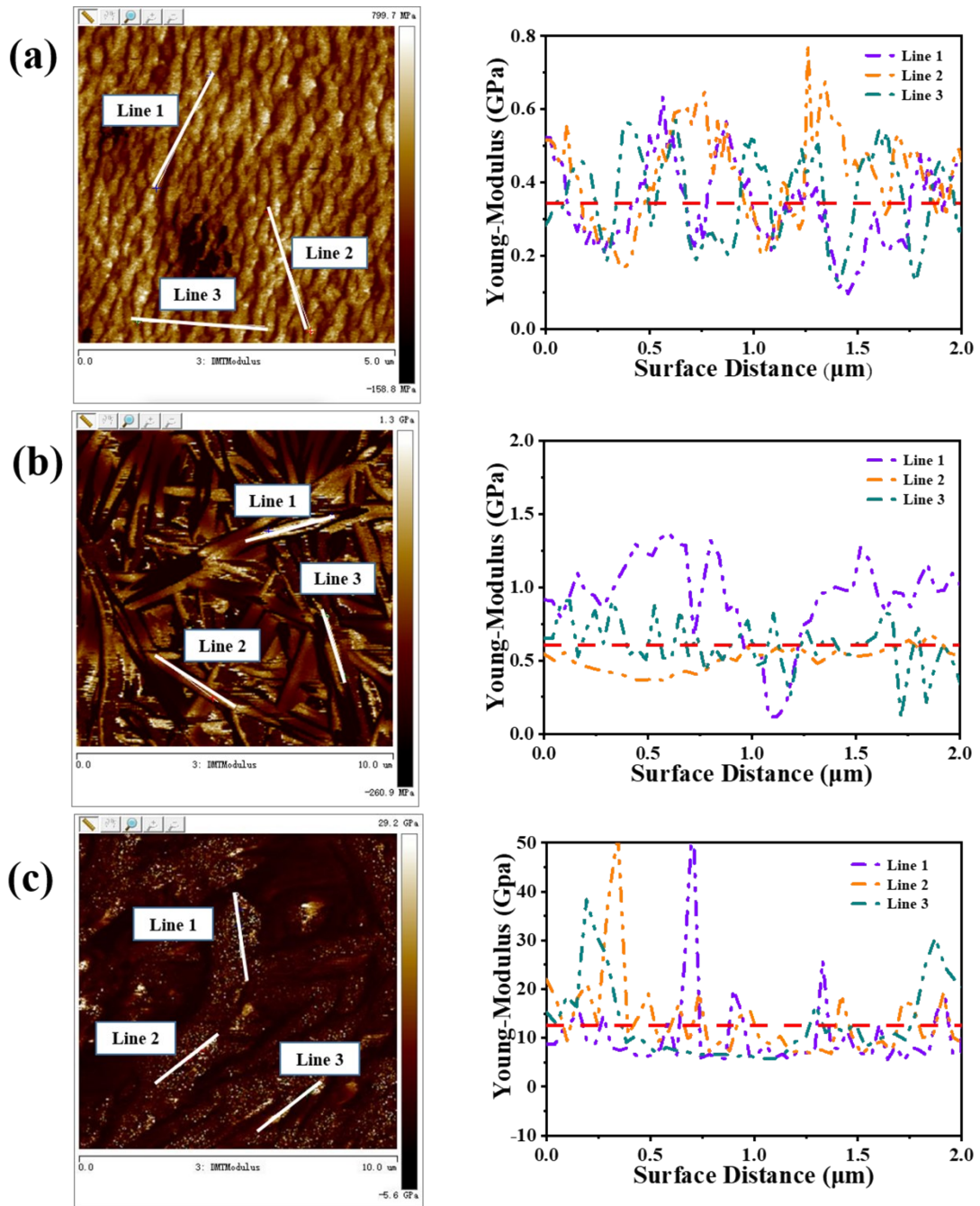


Figure S14. The Young's modulus mapping and corresponding partial modulus in detail of (a) Celgard separator, (b) PVA separator and (c) P@S-25 separator.

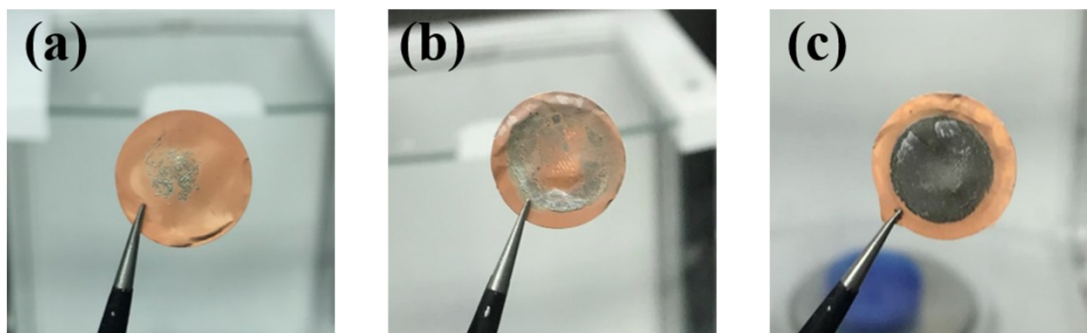


Figure S15. Digital pictures of Cu foil after the first cycle lithium metal deposition by using different separator at the current density of $1.0 \text{ mA}\cdot\text{cm}^{-2}$ for 1 h. (a) Celgard separator, (b) PVA separator and (c) P@S-25 separator.

Table S1. Physical and electrochemical properties of the Celgard, PVA, P@S-10, P@S-25 and P@S-50 separators

| Samples | Thickness (μm) | Ionic conductivity (mS cm^{-1}) | Porosity (%) | Uptake (%) |
|----------------|---|--|-------------------------|-----------------------|
| Celgard | 25.0 \pm 2.00 | 0.1527 \pm 0.0012 | 50.04 \pm 2.95 | 80.30 \pm 5.65 |
| PVA | 23.75 \pm 1.75 | 0.2737 \pm 0.0201 | 57.80 \pm 4.52 | 348.70 \pm 17.47 |
| P@S-10 | 25.64 \pm 3.03 | 0.5607 \pm 0.0662 | 59.88 \pm 3.45 | 375.50 \pm 9.47 |
| P@S-25 | 25.94 \pm 3.33 | 1.0835 \pm 0.0589 | 62.28 \pm 2.85 | 410.31 \pm 6.78 |
| P@S-50 | 26.88 \pm 3.80 | 1.4231 \pm 0.0813 | 65.80 \pm 2.85 | 467.69 \pm 21.52 |